

## ARTEMISS – an Algorithm to Retrieve Temperature and Emissivity from Hyper-Spectral Thermal Image Data

**Christoph C. Borel**

Los Alamos National Laboratory, Los Alamos, NM 87545  
505-667-8972 / [cborel@lanl.gov](mailto:cborel@lanl.gov) / <http://nis-www.lanl.gov/~borel>

### Abstract

*ARTEMISS (Automatic Retrieval of Temperature and Emissivity using Spectral Smoothness), is a method based on (1) in-scene atmospheric transmission estimation, (2) matching of the transmission to a database and (3) retrieving a spectrally smooth emissivity by an iterative method is used on hyper-spectral data.*

### 1. INTRODUCTION

#### 1.1 Multi-spectral Temperature-Emissivity Separation

The central problem of temperature-emissivity separation is, as pointed out by Realmuto, 1990, that we obtain  $N$  spectral measurements of radiance and need to find  $N+1$  unknowns ( $N$  emissivities and one temperature). In the past, several methods (Assumed channel 6 emittance model: Kahle et al., 1980; Emissivity Spectrum Normalization (ESN): Realmuto, 1990; thermal log and alpha residual: Hook et al., 1992 and Mean-Maximum Difference (MMD): Matsunaga, 1993) have been developed to retrieve surface emissivity and temperature from multi-spectral data (TIMS).

#### 1.1 Hyper-spectral Temperature-Emissivity Separation

Hyper-spectral data in the thermal regime requires different processing from the processing done of hyper-spectral data in the reflective regime. Rather than just retrieving the surface reflectance as in the 0.4 to 2.5 micron region, we must also take into account the self-emission due to radiation of the surface at some temperature  $T$  which is modulated by the emissivity of the material. For low emissivity materials, the surface-leaving radiance contains also a reflected down-welling component. The intervening atmosphere absorbs some of the surface leaving radiance and adds path radiance. To analyze hyper-spectral thermal data, it is thus necessary to correct the data for the atmospheric effects to retrieve surface emissivity and temperature. This process is commonly called temperature/emissivity separation (TES) and only a few algorithms exist for hyper-spectral data. One is the In-Scene Atmospheric Correction (ISAC) algorithm by Johnson and Young, 1998 and 2002 and the other we know of is the Autonomous Atmospheric Compensation by Gu et al, 1999. In 1996 we found that we could vary the atmospheric parameters such as water vapor and atmospheric temperature and also vary surface temperature in small steps to compute the emissivity. When the surface temperature is just right the emissivity is smooth, i.e. has no atmospheric features present.

### 2. In-Scene Atmospheric Correction

Typical scenes are composed of many materials with different emissivities and temperatures. In the thermal region, there are many materials such as water, vegetation and certain rough surfaces (where multiple reflections occur) which have a high and featureless emissivity spectrum. Thus, these surfaces behave almost as blackbodies. The ISAC method can be broken down into the following sequence of steps:

1. We select a wavelength  $\lambda_0$  such that the transmission through the atmosphere is high ( $\tau \sim 1$ ) and the path radiance is negligible ( $L_p \sim 0$ ).

2. The ISAC method assumes that the emissivity  $\varepsilon(\lambda) = \varepsilon_0$  has a constant value (e.g.  $\varepsilon_0 = 0.95$ ), thus we can compute the apparent brightness temperature:

$$T_B(i,j) = BB^{-1}(\lambda_0, L_m(\lambda_0, i,j)) / \varepsilon_0$$

of a surface from the inverse Planck function.

3. For another spectral region where the atmosphere is not as transparent, we measure the radiance:

$$L_m(\lambda, i,j) = B(\lambda, T_B(i,j))\tau + L_p.$$

A scatter plot of the computed radiance  $B(\lambda, T_B(i,j))$  on the X-axis and the measured radiance  $L_m(\lambda, i,j)$  on the Y-axis for all pixels  $(i,j)$  shows typically a pattern as shown in Figure 1. The highest points for a given bin on the X-axis correspond to pixels which originate from blackbody-like surfaces. Points below appear cooler than what one would expect from the estimate at wavelength  $\lambda_0$  and thus originate from surfaces where the emissivity is smaller than unity (graybody).

4. Next we fit a straight line to the upper boundary of the points for many bins along the X-axis and from the simple linear model for the radiance of a blackbody at the sensor, we find then that the slope is proportional to the transmission  $\tau(\lambda)$  and the intercept ( $B(\lambda, 0) = 0$ , where the surface temperature is zero) is proportional to the path radiance  $L_p$ . By performing this fitting for each wavelength  $\lambda$ , we derive a transmission spectrum which looks like an atmospheric transmission spectrum. A feature of the spectrum is that the transmission is unity and the path radiance is zero for  $\lambda = \lambda_0$ . If there are other wavelengths where the transmission is higher than at  $\lambda_0$ , then the estimated transmission will rise above unity which, of course, is physically impossible. Similarly, it can then happen that the estimated path radiance is negative. Schemes (Johnson and Young, 1998) exist to iteratively fix the transmission and path radiance to make them physically realistic.
5. The emissivity retrieved by the ISAC method is then given by:  $\varepsilon(\lambda, i,j) = [L_m(\lambda, i,j) - L_p(\lambda)] / [B(\lambda, T_B(i,j))\tau(\lambda)]$ .

We found, however, that there will always be small differences introduced in spectral regions where no blackbody-like surfaces exist. Also if the temperature range of the scene is small, e.g. under night time conditions, the fitting of a line produces noisy slopes and offsets.

It is important to remember that the ISAC method assumes high emissivities in general, and thus neglects the reflected down-welling radiance in the full radiative transfer equation. For an arbitrary surface emissivity we need to consider the reflected down-welling sky radiance  $L_d$ :

$$L_m = \varepsilon B(\lambda, T) \tau + (1 - \varepsilon) L_d \tau + L_p. \quad (1.1)$$

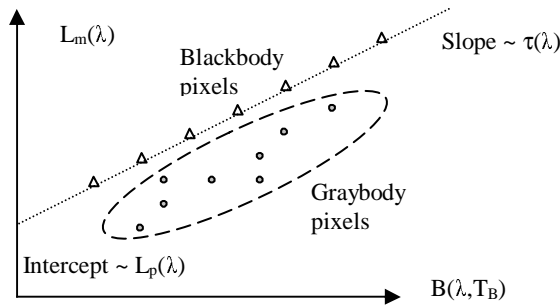


**Figure 1 In-Scene Atmospheric Correction using regressions**

### 3. Surface Emissivity and Atmospheric Transmission

It is a common observation that thermal-infrared spectra of solids are much smoother than thermal-infrared spectra of gases. This difference is due to the fact that spectral features of solids tend to be fairly wide, whereas those in a gas tend to be narrower. The width of a given spectral feature is inversely proportional to the lifetime of the transition which created it - short lifetimes give wide features whereas long lifetimes create narrow features. In a solid, the individual molecules are bound together, creating a coupled and highly complex vibrational system. As a result, the lifetimes of excited states tend to be short because they get disrupted by thermal motions (or "phonons") within the crystal lattice. In a gas, however, the individual molecules are isolated and tend to be simpler. There are thus fewer potential phenomena to disrupt an excited state, resulting in longer lifetimes and narrower spectral features.

### 4. Spectrally Smooth Emissivity Retrieval Algorithm

The main idea is that we can solve the equation for the measured path radiance  $L_p$  for the unknown emissivity  $\varepsilon$  using an estimate of the blackbody ground temperature  $T_{est}$  derived in an atmospheric window assuming a "typical" emissivity of  $\varepsilon_0=0.95$ . Then we vary the blackbody temperature in a range of temperatures near  $T_{est}$  and compute the emissivity  $\varepsilon(\lambda)$ . Iteratively we compute the smoothness of the spectral emissivity and select the smoothest emissivity as the best estimate  $\varepsilon_{opt}(\lambda)$ .

We found this method to produce very reasonable results under the condition that we also need to vary the atmospheric temperature  $T(\lambda)$ , cumulative water vapor and ozone amount to bring the estimated emissivities close to well known emissivities such as that of water. In Figure 2 we show emissivities of various natural surface types (Salisbury, 1992). Note that they tend to reach high emissivities in the 11.5-12.5  $\mu\text{m}$  region.

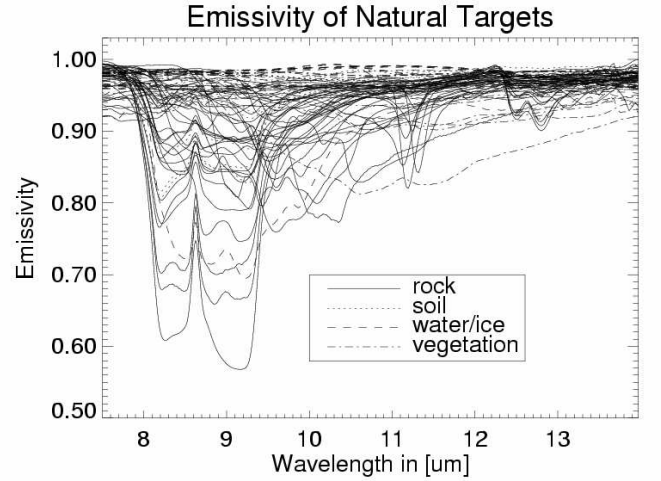


**Figure 2 Emissivities of various natural surfaces from Johns Hopkins spectral library**

Now a more detailed description of the algorithm includes the following steps:

1. Solve eq. (1.1) for  $\varepsilon$ :

$$\varepsilon = \frac{L_m - L_p - L_d \tau}{(B(\lambda, T_{est}) - L_d) \tau}, \quad (1.2)$$

where the estimated ground temperature  $T_{est}$  is given by:

$$T_{est} = B^{-1} \left( \lambda_0, \frac{L_m - L_p - (1 - \varepsilon_0) L_d \tau}{\varepsilon_0 \tau} \right), \quad (1.3)$$

where  $\lambda_0$  is a wavelength where the atmosphere is highly transmissive and  $\varepsilon(\lambda)$  is typically set to 0.95. Using eq. (1.3) in (1.2) usually results in an emissivity spectrum which shows some atmospheric line features.

2. To get rid of the atmospheric features we search for a temperature offset  $\Delta T$  such that the emissivity  $\varepsilon_{opt}(\lambda)$  becomes smooth. A good criterion for smoothness is the standard deviation  $\sigma$  of the difference between the computed emissivity  $\varepsilon_{opt}(\lambda)$  and a boxcar averaged version of  $\varepsilon_{opt}(\lambda)$  is minimized. In other words, we search a  $\Delta T$  such that the following equation is minimized:

$$\sigma(\Delta T) = \text{STDEV}[\varepsilon(\lambda) - \text{smooth}(\varepsilon(\lambda), 3)], \quad (1.4)$$

where STDEV is the standard deviation and smooth is a 3-point average of the emissivity.

3. A problem is that the up- and down-welling path radiances and transmission are usually not known unless a radiosonde was launched at the time of the measurement recording the temperature and humidity profile. To find the correct atmosphere is a crucial step for the smooth emissivity retrieval to work. If the wrong temperature or humidity profile is used, we find that the

emissivities are shifted and the retrieved temperature is offset from the true temperature. If we know what the emissivity is for a given region in the data, then we can determine the necessary offsets in temperature and emissivity to correct the data.

#### 4.1 A Method to Find the Best Atmosphere

The retrieved emissivity is only usable if we can find an atmosphere which is very close to the actual conditions. For high resolution (e.g. better than  $1 \text{ cm}^{-1}$  sampling), it is possible to invert measured radiance spectra of the broad-band sky radiance in atmospheric windows by (e.g. AERI instrument of the University of Wisconsin). These high spectral resolution instruments use line broadening to estimate the temperature at different altitudes. Dispersive imaging sensors rarely achieve a resolution finer than 2-3 wavenumbers. The coarse spectral resolution makes it impossible to measure line broadening. Imaging spectrometers are used to sense the Earth's surface and are thus restricted to atmospheric windows, e.g. from 7.5 to  $13.5 \text{ }\mu\text{m}$ . Furthermore, the background is the Earth's surface which is almost always warmer than the atmosphere. Thus, atmospheric features appear in absorption rather than emission as with sky radiance measurements, which in turn makes it harder to estimate the atmospheric temperature. The cumulative water vapor in the atmosphere is also highly variable on scales of  $10^3$ 's of kilometers. Ozone is another gas which can vary from region to region and needs to be corrected for data from sensors flying above 10 km altitude.

Originally, we tried to perform the temperature emissivity separation using a simple 1-layer model for the atmosphere (Borel, 1997). Since the absorption due to water vapor is highly non-linear and does not follow the exponential Beer's Law, it is necessary to use more accurate data. One of the most advanced codes for the spectral regime and resolution of interest is MODTRAN from the Air Force Research Laboratory (Berk et al, 1999). This code allows the atmosphere to be specified in N layers with different temperatures and relative humidities with many other options such as aerosol models, other gas concentrations, etc. The output contains the necessary elements which we call the TUD (for transmission, up-welling, down-welling radiance) for ARTEMIS: (1) transmission  $\tau(\lambda)$ , (2) path radiance  $L_p(\lambda)$  and (3) down-welling radiance  $L_d(\lambda)$ .

The algorithm described above is simple except that there are potentially many atmospheres giving a smooth but physically incorrect emissivity. A major practical problem is the efficient searching for the correct atmosphere. Until now we have used look-up table (LUT) to store the TUD which often contains hundred to thousands of atmospheric cases. To find the best candidate atmosphere from the LUT we found that the ISAC method provides a good first estimate of the atmospheric transmission. Thus, we devised a hybrid algorithm which we call ARTEMIS which uses ISAC as a first step to find a number of candidate atmospheres, based on a simple criterion such as maximizing the  $R^2$  in a linear regression or the cosine of the spectral angle when performing the vector dot product of the estimated transmission with a LUT transmission. For each of the candidate atmospheres, the smooth emissivity retrieval method is applied in M randomly or from a spectral angle classification

chosen test pixels. A counter for the atmospheric case with the smallest  $\sigma$  is updated for each test pixel. The atmospheric case with most votes is declared a winner. Finally the full entries from the TUD-LUT ( $L_p$ ,  $L_d$  and  $\tau$ ) are then used to retrieve the temperature and emissivity for all pixels using the smooth emissivity retrieval.

In Figure 3 we show a series of curves of retrieved emissivities when the temperature is varied. Notice that the atmospheric absorption/emission features seem to disappear when the retrieved emissivity is smooth. In Figure 4 we show how the smoothness varies as a function of temperature offset  $\Delta T$ . Note the sharp minimum will be filled in if there is a difference between actual and assumed atmosphere, sensor noise and spectral shifts.

In Figure 5 we show a flow diagram of the simulation software we developed to compute the sensitivity of the temperature emissivity separation result to atmosphere and sensor changes. Since data from current sensors is not "perfect" we found that it is necessary to use simulated data. With this simulation system we can study many different sensor configurations and compare algorithm variations to find an optimum combination to achieve a certain performance.

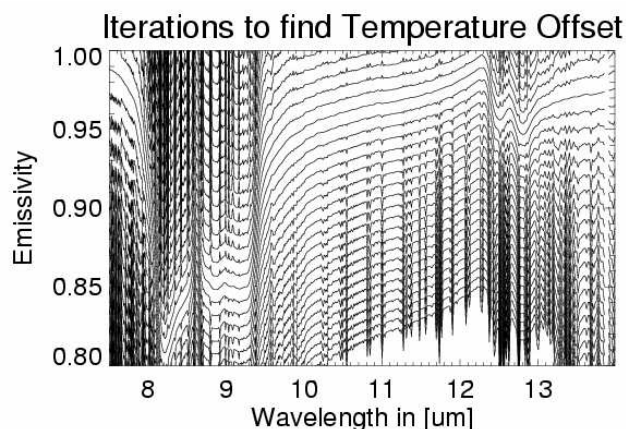


Figure 3 Smooth emissivity retrieval using different temperature offsets from -10 to 10 K in steps of 0.5 K.

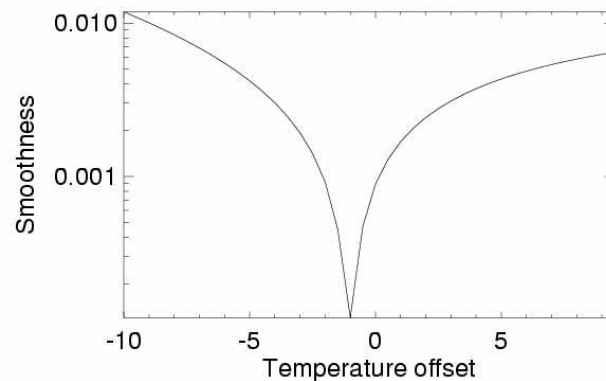
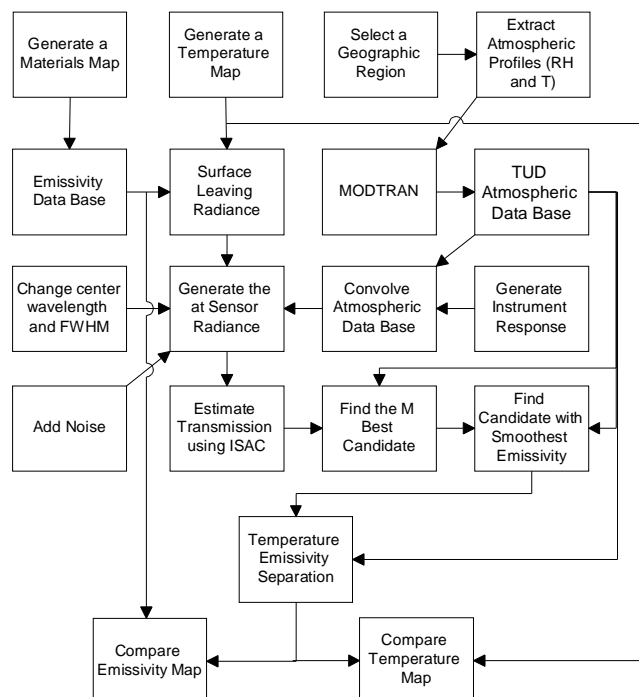


Figure 4 Smoothness as a function of temperature offset  $\Delta T$



## 5. Conclusions

Hyperspectral sensors with 100 or more channels are necessary to accurately retrieve temperature, emissivities and atmospheric parameters. A new hybrid method has been developed which uses the smoothness of the spectral emissivity to retrieve temperature and emissivity. A good atmospheric correction is a necessary condition to retrieve accurate surface temperatures and emissivities.

In the future we need to perform a sensitivity study to investigate the effect due to calibration errors (spectral and radiometric) and sensor noise. We need to investigate the problem of mixed pixels and potentially devise nonlinear un-mixing methods. We should study the use of low-emissivity surfaces to retrieve down-welling path radiances.

## 6. ACKNOWLEDGEMENTS

Our thanks go to the Air Force Research Laboratory, Hanscom AFB, MA, which supported this research during my year as a distinguished national laboratory fellow. I worked closely with Dr. Ronald Lockwood and Dr. Michael Hoke both from AFRL. Many fruitful discussions with Dr. Bradley Henderson, Dr. Steve Love and Dr. William Clodius - all in NIS-2, LANL and Dr. Marsha Fox and Dr. Larry Bernstein from Spectral Sciences Inc, Burlington, MA.

## 7. References

[1] A. Berk , G. P. Anderson, L. S. Bernstein, P. K. Acharya, H. Dothe, M. W. Matthew, S. M. Adler-Golden, J. H. Chetwynd, Jr., S. C.

Richtsmeier, B. Pukall, C. L. Allred, L. S. Jeong, and M. L. Hoke, "MODTRAN4 Radiative Transfer Modeling for Atmospheric Correction," SPIE Proceeding, Optical Spectroscopic Techniques and Instrumentation for Atmospheric and Space Research III, Volume 3756 (1999).

[2] Borel, C.C, Iterative Retrieval of Surface Emissivity and Temperature for a Hyperspectral Sensor, *First JPL Workshop on Remote Sensing of Land Surface Emissivity*, May 6-8, 1997. (available only from authors website <http://nis-www.lanl.gov/~borel>)

[3] Gu, D., A.B. Kahle and Palluconi F.D, Autonomous Atmospheric Compensation (AAC) of high-resolution hyperspectral thermal infrared remote-sensing imagery, *IEEE Trans. Geosci. Remote Sensing*, 38(6), 2557-2570, 1999.

[4] Hook S.J., A.R. Gabell, A.A. Green and P.S. Kealy, A comparison of techniques for extracting emissivity information from thermal infrared data for geologic studies. *Remote Sens. Environ.*, 42, 123-135, 1992.

[5] Johnson, B.R. and S. J. Young, Inscene Atmospheric Compensation: Application to SEBASS Data at the ARM Site, *Aerospace Report* No. ATR-99(8407)-1 Parts I and II,(1998).

[6] Kahle, A.B., D.P. Madura and J.M. Soha, Middle Infrared Multispectral Aircraft Scanner Data: Analysis for Geologic Applications. *Applied Optics*, 19(14):2279-2290, 1980.

[7] Matsunaga, T., An Emissivity-Temperature Separation Technique Based on an Empirical Relationship Between Mean and Range of Spectral Emissivity, *Proc. 14th Japanese Conf. of Remote Sensing*, 47-48, 1993.

[8] Realmuto, V.J., Separating the Effects of Temperature and Emissivity: Emissivity Spectrum Normalization, Proc. of the Second TIMS Workshop, *JPL Publ.* 90-55, 31-35, 1990.

[9] Salisbury, J. W. and D. M. D'Aria, Emissivity of Terrestrial Materials in the 8-14  $\mu\text{m}$  Atmospheric Window, *Remote Sens. Environ.*, 42, 83-106, 1992.

[10] Young, S. J., Detection and Quantification of Gases in Industrial-Stack Plumes Using Thermal-Infrared Hyperspectral Imaging, *The Aerospace Corporation Report No. ATR-2002(8407)-1*.

## 8. BIBLIOGRAPHY

Christoph C. Borel received a diploma in electrical engineering (Dipl. El. Ing. ETH) in 1981 from the Swiss Federal Institute of Technology (ETH) in Zurich, Switzerland. From 1981-1983 he held a research position with the Institute of Communication Technology at the ETH., where he worked on simulating and characterizing fiber optic transmission systems. In the fall of 1983 he joined the Microwave Remote Sensing Laboratory (MIRSL) of the University of Massachusetts, Amherst, MA. He received a Ph.D. in electrical and computer engineering from UMass in 1988 with a thesis on scattering models of vegetation in the millimeter wave region. In 1988 he joined the Theoretical Division of the Los Alamos National Laboratory in Los Alamos, NM. As a postdoctoral fellow he worked on the implementation of the radiosity theory for remote sensing applications, design and construction of an artificial canopy and atmospheric correction algorithms. In 1990 he joined the Space Science and Technology which later became the Non-proliferation and International Security Division as a staff member. His current research interests are vegetation modeling in the visible and infrared using the radiosity method, computer graphics algorithms, image analysis, hyper-spectral image analysis and synthesis, and atmospheric corrections.